Coexistence of antiferromagnetic and ferromagnetic orders at remanent state in epitaxial multiferroic Bi_2FeCrO_6 nanostructures

2012 J. Phys.: Condens. Matter 24 142202

(http://iopscience.iop.org/0953-8984/24/14/142202)

IOP FTC
IOP PUBLISHING JOURNAL OF PHYSICS: CONDENSED MATTER
J. Phys.: Condens. Matter **24** (2012) 142202 (5pp) doi:10.1088/0953-8984/24/14/142202

FAST TRACK COMMUNICATION

Coexistence of antiferromagnetic and ferromagnetic orders at remanent state in epitaxial multiferroic Bi_2FeCrO_6 nanostructures

R Nechache[1,2], C Nauenheim[2], U Lanke[3], A Pignolet[2], F Rosei[2,4] and A Ruediger[2]

[1] NAST Center and Department of Chemical Science and Technology, University of Rome Tor Vergata, Via della Ricerca Scientifica 1, I-00133 Rome, Italy
[2] INRS–Énergie, Materiaux et Télécommunications, Université du Québec, 1650 Boulevard Lionel Boulet J3X 1S2 Varennes, QC, Canada
[3] Canadian Light Source Inc., 101 Perimeter Road Saskatoon, SK S7N 0X4, Canada
[4] Centre for Self-Assembled Chemical Structures, McGill University, 801 Sherbrooke Street West, H3A 2K6 Montréal, QC, Canada

E-mail: ruediger@emt.inrs.ca

Received 11 January 2012, in final form 17 February 2012
Published 5 March 2012
Online at stacks.iop.org/JPhysCM/24/142202

Abstract
We report the local electronic and magnetic properties of Bi_2FeCrO_6 nanostructures by element-specific polarized x-ray techniques. Sizable magnetic ordering in the remanent state is observed at room temperature for both Fe and Cr ions. The Bi_2FeCrO_6 system offers an example of d^5–d^3 magnetic superexchange interaction with a magnetic order for both Fe and Cr, which are both formally in the +3 valence state. The results suggest a coexistence of antiferromagnetic and ferromagnetic superexchange interaction between Fe and Cr spins in the nanostructures at the remanent state and at room temperature.

(Some figures may appear in colour only in the online journal)

1. Introduction

Bi-based multiferroic double perovskites, $Bi_2BB'O_6$, in which two different B-site cations form a superlattice within the ABO_3 perovskite structure, have recently attracted substantial interest [1]. Because of their multi-functionality, these materials are promising for breakthroughs in emerging fields such as spintronics and data storage technology [2, 3]. The successful growth of Bi_2FeCrO_6 (BFCO), a double perovskite with functional properties well above room temperature, opens opportunities for practical applications of multiferroics [4, 5]. BFCO films have a similar crystal structure as $BiFeO_3$ (BFO) and exhibit a Fe^{3+}–Cr^{3+} ordering along the (111) direction, offering an example of d^5–d^3 magnetic superexchange interaction [5]. Recent works demonstrated that an ordered BFCO phase can be obtained both in thin film and nanostructured forms by using conventional pulsed laser deposition (PLD) [6–8]. The existence of Fe–Cr cation ordering in BFCO has been evidenced by x-ray diffraction (XRD) and electron diffraction by the observation of superlattice peaks [9]. Furthermore, by stacking alternating monolayers of stoichiometric BFO and $BiCrO_3$ on 111-oriented $SrTiO_3$ (STO) substrates, Ichikawa *et al* have artificially grown BFCO films with rock salt structure B-site ordering [7]. The existence of a large ferroelectric polarization in BFCO was independently

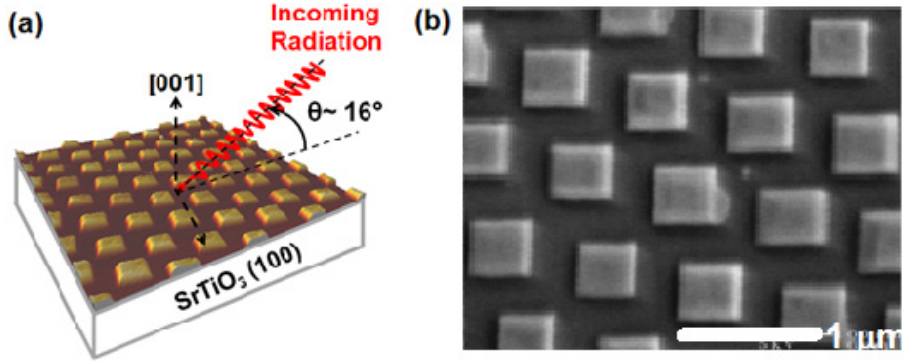

Figure 1. (a) AFM topography image of BFCO nanostructures grown on STO substrate and XPEEM experimental geometry. (b) SEM image showing the square shape of the submicron BFCO structures.

confirmed by all these studies as well as a strong magnetism at room temperature (RT). In particular, magnetic measurements revealed a maximum magnetization of 1.9 [9], 5.2 [10] and 3.4 μ_B/f.u. [7] for BFCO thin films, nanostructures and artificial superlattices, respectively. These results have been explained by a ferro/antiferromagnetic coupling within Fe–O–Cr bonds, depending on the strength and angle of the superexchange interaction between the Cr^{3+} and Fe^{3+} cations [9]. The reported magnetic values raise questions concerning the nature of the ordered magnetic state in the BFCO system.

Here, we report the local electronic and remanent magnetic properties of Bi_2FeCrO_6 nanostructures by element-specific polarized x-ray techniques. Sizable magnetic ordering in the remanent state is observed at room temperature for both Fe and Cr ions. The BFCO system offers an example of d^5–d^3 magnetic superexchange interaction with a magnetic order for both Fe and Cr, which are both formally in the +3 valence state. The results suggest predominance at remanence of antiferromagnetic superexchange interaction between Fe and Cr spins in the nanostructures with weak indications of ferromagnetism.

2. Experimental details

The nanopatterning of BFCO was obtained by PLD through nanostencil shadow masks [11–13]. The deposition parameters for the growth of the epitaxial BFCO nanostructures were reported elsewhere [10]. The nanostructures exhibit a square-like shape with an average width of 400 nm and a height of about 25 nm (see figure 1(b)). The global saturation and remanent in-plane magnetizations were about 5.2 and 1.0 μ_B/formula unit (f.u.), respectively (corresponding to 2.7 and 0.45 μ_B/cation)[5,6].

We investigated the local electronic and magnetic properties of BFCO nanostructures using the element-specific techniques, x-ray absorption (XAS) and x-ray magnetic circular dichroism (XMCD) spectroscopies, after the sample had previously been magnetized in the course of VSM characterization [10]. X-ray photoemission microscopy (XPEEM) measurements were performed at the spectromicroscopy (SM) beamline at the Canadian Light Source (CLS). The beamline is equipped with a APPLEII type elliptically polarized undulator (EPU) that can deliver polarized photons. The low-energy secondary photoelectrons from the sample are imaged by PEEM optics consisting of a series of electro-magnetic lenses with final magnification onto a phosphor screen read by a charge-coupled device (CCD) camera. For an ideal flat sample, the spatial resolution of the PEEM microscope is better than 30 nm. All the XPEEM measurements were done without magnetic field, we are thus detecting the remanent part of the BFCO magnetization at room temperature.

3. Results and discussion

XAS/XMCD is defined as the sum/difference between the absorption spectra for left-polarized and right-polarized x-rays [14, 15]. The polarized x-ray beam impinged on the sample at an angle of 16° (see figure 1(a)). The beam polarization is switched between left-circularly (LCP) and right-circularly (RCP) polarized light at each energy interval to measure the magnetization, parallel (M^+) and anti-parallel (M^-) to the photon chirality. XAS ($M^+ + M^-$) reveals the electronic character of a particular element in its environment, while XMCD ($M^+ - M^-$) probes the element-specific net magnetization. By tuning the photon energy to either the Fe L-edge, near 710 eV, or the Cr L-edge, near 578 eV, we recorded separate images and estimated the individual contributions of Fe and Cr to the remanent magnetic moment of the BFCO nanostructures. The LCP and RCP PEEM images obtained for Fe and Cr exhibit in general a uniform contrast in the nanostructured region (see figures 2(a), (b), (d) and (e)).

The XMCD contrast at the Fe L-edge is stronger than and mainly anticorrelated to that of the Cr L-edge (see figures 2(c) and (f)). Our sample is insulating and therefore not ideal for an electron microscopy investigation which is prone to surface

[5] The in-plane magnetization of the submicron nanostructures was measured with an applied magnetic field parallel to the surface using a vibrating sample magnetometer with a sensitivity of 10^{-6} emu.

[6] The use of nanostructured BFCO on a conducting substrate effectively prevents surface charging effects under XPEEM conditions.

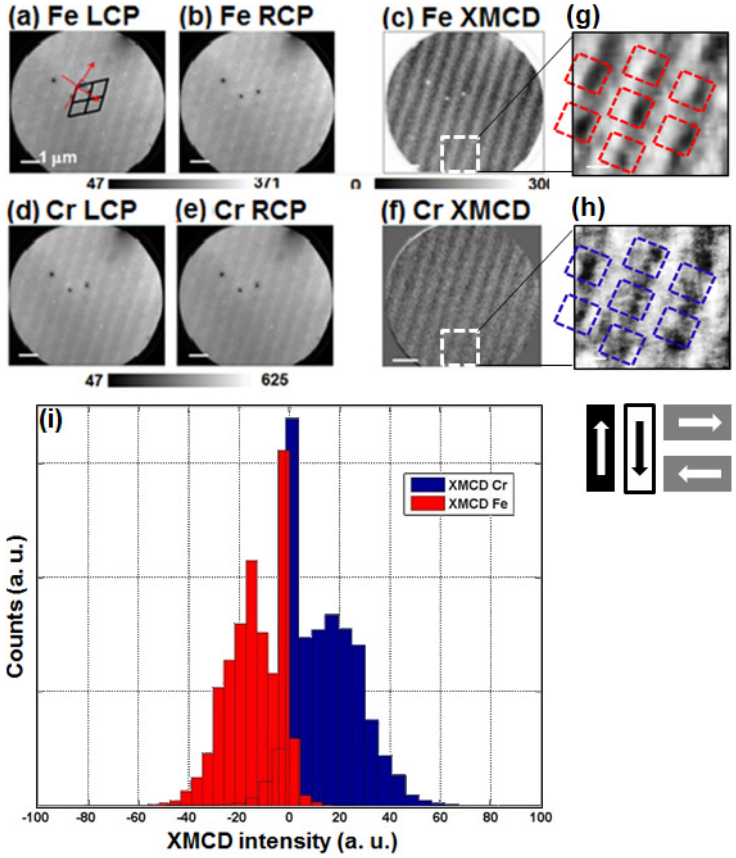

Figure 2. XPEEM images at RT and zero magnetic field obtained for both Fe and Cr cations: left circular polarization (LCP) for (a) Fe and (d) Cr; right circular polarization (RCP) for (b) Fe and (e) Cr. XMCD images for (c) Fe and (f) Cr, respectively. (g), (h) Enlarged area images, scale bar = 250 nm. Magnetic domains with in-plane orientations of the magnetic spins are indicated in the images. Squares represent positions of the nanostructures. (i) Distribution histogram of Fe and Cr XMCD intensities extracted from the images (c) and (f). The high peak around the zero XMCD signal originates from the $SrTiO_3$ substrate. The curves being mostly negative for Fe and mostly positive for Cr indicate a preferential antiferromagnetic ordering with a small ferromagnetic contribution where both distributions overlap. The gray background in images (a), (b), (d) and (e) originates from the substrate. The hexagonal pattern of the nanostructures is indicated in black in (a) and red arrows represent the in-plane cubic crystal directions.

charging effects that significantly reduce the resolution[7]. As to the element contrast, it is not weak, but appears weak due to the dynamic range that includes three inactive pixels. The histogram underlines the good quality of our data. An example of XPEEM images from an enlarged region are given in figures 2(g) and (h). We can distinguish a contrast from magnetic domain structures. In our experimental geometry, we were not able to distinguish left from right horizontally oriented domains (gray color) but we resolved domains aligned vertically up (black) and down (white). From figures 2(g) and (h), the in-plane projection of Cr and Fe spins can be anti-parallel, parallel and perpendicular. A more detailed analysis of the images (i.e. histogram distribution, figure 2(i)) confirms this possible coexistence of ferromagnetic (FM) and antiferromagnetic (AFM) ordering of Fe and Cr spins in the BFCO nanostructures. However, from the histogram of Cr/Fe XMCD intensity distribution deduced from the overall analyzed area, we conclude that the spins are predominantly antiferromagnetically coupled in the remanent state and at RT (see figure 2(i)).

Spectra were also recorded at RT in the total electron yield mode at the Fe and Cr L-edges without applying an external magnetic field. The beamline energy resolution is better than 0.1 eV at around 700 eV. Figure 3 shows the absorption spectra at the Fe and Cr L-edges for the two photon chirality (M^+, M^-), and the corresponding XAS and XMCD spectra. The XPEEM spectra (M^+ and M^-), which result from the (Fe/Cr) 2p–3d dipole transition, are roughly divided into the L_3 ($2p_{3/2}$) and L_2 ($2p_{1/2}$) regions (see figures 3(a) and (d)).

The Fe and Cr XAS spectra illustrated in figures 3(b) and (e) are analogous to those of Fe^{3+} (α-Fe_2O_3) and Cr^{3+} (Cr_2O_3) standards [16, 17]. The strong similarity of spectral features between the BFCO nanostructures and α-Fe_2O_3 for the Fe cation suggests an analogue local electronic environment. The Fe in α-Fe_2O_3 has an octahedral symmetry O_h (Fe is surrounded by six oxygen atoms) with a crystal field splitting (10Dq) of 1.45 eV. Fe is in a high spin state configuration $t_{2g}^3e^2$ with a valence state of +3 [18]. Furthermore, the XMCD spectrum of γ-Fe_2O_3 [19], which

[7] Even an ideal resolution should have provided nothing better than a 400 nm sample width/30 nm resolution = 13 pixels per islands. We obtained roughly 10 pixels per islands.

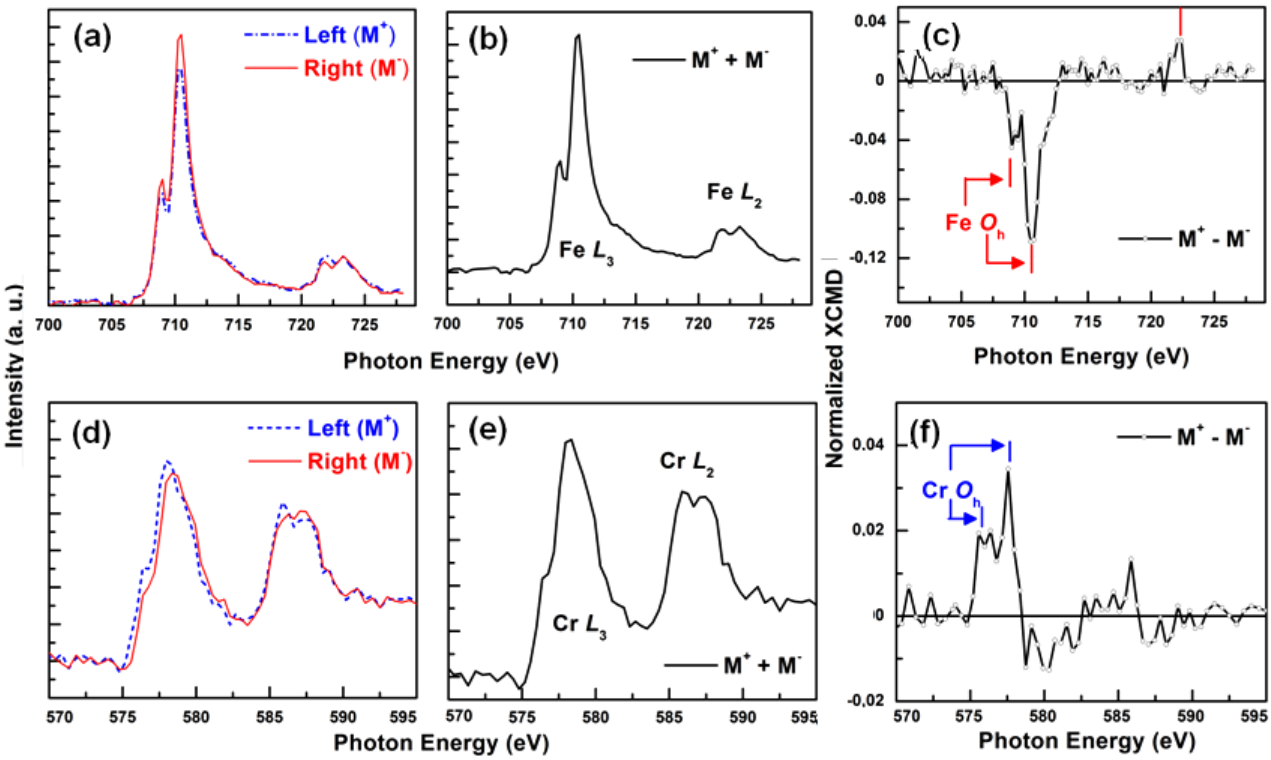

Figure 3. XPEEM local spectra for (a) Fe L-edges and (d) Cr L-edges. Corresponding XAS/XMCD spectra for Fe ((b)/(c)) and Cr ((e)/(f)). The XMCD intensities were normalized by the intensities of the XAS peaks.

displays the sum of the contributions from the T_d and O_h sites, is completely different from that of BFCO that displays only the contribution from the O_h sites (see figure 3(c)).

For the Cr cation, the comparison between Cr L (see figure 3(e)) of the nanostructures and the calculated spectrum of chromium oxide (Cr_2O_3) indicates that the state of Cr in the as-grown nanostructure is a high spin state t_{2g}^3 and a valence state of +3. Cr_2O_3 has a crystal field splitting of 2.0 eV with a small distortion from the octahedral symmetry [15].

From the normalized XMCD of both Fe and Cr $L_{3,2}$ edges, the opposite polarities of Fe and Cr can be distinguished on the two spectra (see figures 3(c) and (f)), revealing a predominantly anti-parallel alignment of the magnetic moments of Fe and Cr in the absence of an applied magnetic field. Fe and Cr exhibit a maximum asymmetry at the L_3 edge of about 10.9% and 3.4%, respectively. For typical ferromagnets with an average magnetic moment of 3–5 μ_B per magnetic site, the expected XMCD signal is 30%–40%.

The magnetic moments can be estimated by weighing the size of the measured XMCD signal against standards of known moments of magnetic cations with the same valence, ligand field symmetry and spectral features [20]. Following this procedure, magnetic moments at remanence of 1.2 ± 0.1 μ_B/Fe and 0.4 ± 0.1 μ_B/Cr were estimated for the BFCO nanostructures. In the magnetic double perovskite, the nucleation of stacking defects such as antisites (AS) and antiphase boundaries (APBs) mainly affect the remanent magnetization [21]. Significant reductions of the remanent magnetization due to the AFM alignment of the adjacent ordered domains separated by APBs were observed in several materials [22, 23]. The remanent magnetization observed in the BFCO nanostructures can thus be described in terms of the formation of APBs at the interface of out-of-phase perfectly ordered Fe/Cr regions. Strong antiferromagnetic Fe–O–Fe and weak Cr–O–Cr interactions across a phase boundary would orient the adjacent ordered domain anti-parallel in zero magnetic field. The residual magnetization gives rise to finite but low remanence, as observed in our case.

The in-plane remanent magnetization globally measured by a vibrating sample magnetometer was determined to be 1.0 ± 0.1 μ_B/f.u.. Assuming that the ground state in the BFCO nanostructure was ferrimagnetic (i.e. AFM coupling between Fe and Cr spins), the remanence in the area measured by XPEEM should be $m_{Fe} - m_{Cr} = 1.2 - 0.4 = 0.8$ μ_B/f.u.. This AFM coupling thus cannot explain alone the observed magnetization in the nanostructures. The coexistence of both AFM and FM, as partially evidenced by XCMD analysis (see figure 2) might describe such a situation. This magnetically inhomogeneous system can be the result of the complex competition in d^3–d^5 superexchange interactions (Goodenough–Kanamori rules) where the coupling due to the pdσ hybridization between the e_g orbitals of the TM ions and the oxygen pσ orbital is FM, while the coupling due to the pdπ hybridization with the t_{2g} is AFM. This superexchange interaction is sensitive to the crystal structure and in particular to the Fe–O–Cr angle. The coexistence of two magnetic phases or at least two magnetic orders has already been observed in such magnetic double perovskites [24].

4. Conclusion

In summary, we investigated the local electronic and magnetic environment as well as the ordering of Fe and Cr cations in BFCO nanostructures by XAS and XMCD. XAS confirms that both Cr and Fe are trivalent and in the high spin state. The observed magnetic moments of Cr and Fe confirm the existence of a superexchange magnetic interaction between the two ions, evidencing the formation of a Fe/Cr cation ordering in the nanostructures. The results indicate, as already suggested in earlier work [10], a possible coexistence of AFM and FM coupling and multiple and complex magnetic domain structures in BFCO nanostructures. XPEEM measurements under magnetic and electrical field are under investigation to explain the complex magnetic domain structure observed in the nanostructures as well as to verify whether the domain's structure is driven by magnetic interaction or/and multiferroic coupling. The size effect on the domain's architecture will also be investigated.

Acknowledgments

We acknowledge financial support from the Canada Foundation for Innovation. AP, FR and AR are supported by discovery grants (NSERC). FR is grateful to the Canada Research Chairs Program for partial salary support. RN is grateful to the joint laboratory on Advanced Materials for Energy, Environment and Health, University of Rome 'Tor Vergata' and INRS-EMT for partial salary support. RN thanks NSERC for partial support of his salary via a post-doctoral fellowship. FR acknowledges support from MDEIE (Quebec) for an international collaboration grant. SL and FR are supported by the Italian Ministry of Foreign Affairs (MAE). AR and FR are grateful to FQRNT for a team grant. PEEM-XMCD measurements were performed at the Canadian Light Source, which is supported by NSERC, NRC, the Canadian Institutes of Health Research, the Province of Saskatchewan, Western Economic Diversification Canada and the University of Saskatchewan.

References

[1] Pickett W E 1998 *Phys. Rev.* B **57** 10613
[2] Zutic I, Fabian J and Das Sarma S 2004 *Rev. Mod. Phys.* **76** 323
[3] Bea H, Gajek M, Bibes M and Barthelemy A 2008 *J. Phys.: Condens. Matter* **20** 434221
[4] Nechache R, Harnagea C, Licoccia S, Traversa E, Ruediger A, Pignolet A and Rosei F 2011 *Appl. Phys. Lett.* **98** 202902
[5] Nechache R, Harnagea C, Pignolet A, Normandin F, Veres T, Carignan L P and Ménard D 2006 *Appl. Phys. Lett.* **89** 102902
[6] Nechache R, Gunawan L, Carignan L P, Harnagea C, Botton G, Ménard D and Pignolet A 2007 *J. Mater. Res.* **22** 2102
[7] Ichikawa N *et al* 2008 *Japan. Appl. Phys. Express* **1** 101302
[8] Nechache R, Harnagea C, Pignolet A, Carignan L P and Ménard D 2007 *Phil. Mag. Lett.* **87** 231
[9] Nechache R, Harnagea C, Carignan L P, Gautreau O, Pintilie L, Singh M P, Ménard D, Fournier P, Alexe M and Pignolet A 2009 *J. Appl. Phys.* **105** 061621
[10] Nechache R, Cojocaru C V, Harnagea C, Nauenheim C, Nicklaus M, Ruediger A, Rosei F and Pignolet A 2011 *Adv. Mater.* **23** 1724
[11] Cojocaru C V, Harnagea C, Pignolet A and Rosei F 2006 *IEEE Trans. Nanotechnol.* **5** 470
[12] Cojocaru C V, Harnagea C, Rosei F, Pignolet A, van den Boogaart M A F and Brugger J 2005 *Appl. Phys. Lett.* **86** 183107
[13] Cojocaru C V, Nechache R, Harnagea C, Pignolet A and Rosei F 2010 *Appl. Surf. Sci.* **256** 4777
[14] de Groot F M F, Fuggle J C, Thole B T and Sawatzky G A 1990 *Phys. Rev.* B **42** 5459
[15] Thole B T, Carra P, Sette F and van der Laan G 1992 *Phys. Rev. Lett.* **68** 1943
[16] Kim J Y, Koo T Y and Park J H 2006 *Phys. Rev. Lett.* **96** 047205
[17] Theil C, van Elp J and Folkmann F 1999 *Phys. Rev.* B **59** 7931
[18] Kuiper P, Searle B G, Rudolf P, Tjeng L H and Chen C T 1993 *Phys. Rev. Lett.* **70** 1549
[19] Brice-Profeta S, Arrioa M A, Tronc E, Menguy N, Letard I, Cartier dit Moulin C, Noguees M, Chanéac C, Jolivet J P and Sainctavit Ph 2005 *J. Magn. Magn. Mater.* **288** 354
[20] Kimura A, Matsuno J, Okabayashi J, Fujimori A, Shishidou T, Kulatov E and Kanomata T 2001 *Phys. Rev.* B **63** 224420
[21] Greneche J M, Venkatesan M, Suryanarayanan R and Coey J M D 2001 *Phys. Rev.* B **63** 174403
[22] Woodward P, Hoffmann R D and Sleight A W 1994 *J. Mater. Res.* **9** 2118
[23] Goodenough J B and Dass R I 2000 *Int. J. Inorg. Mater.* **2** 3
[24] Kazan S, Mikailzade F A, Özdemir M, Aktaş B, Rameev B, Intepe A and Gupta A 2010 *Appl. Phys. Lett.* **97** 072511